Published August 2, 2018

Adapting the CROPGRO Model to Simulate Alfalfa Growth and Yield

Wafa Malik,* Kenneth J. Boote, Gerrit Hoogenboom, José Cavero, Farida Dechmi

ABSTRACT

Despite alfalfa's global importance, there is a dearth of crop simulation models available for predicting alfalfa growth and yield with its associated composition. The objectives of this research were to adapt the CSM-CROPGRO Perennial Forage Model for simulating alfalfa growth and yield and to describe model adaptation for this species. Data from six experimental plots grown under sprinkler irrigation in the Ebro valley (Northeast Spain) were used for model adaptation. Starting with parameters for *Bracharia brizantha*, the model adaptation was based on values and relationships reported from the literature for cardinal temperatures and dry matter partitioning. A Bayesian optimizer was used to optimize temperature effects on photosynthesis and daylength effects on partitioning and an inverse modeling technique was employed for nitrogen fixation rate and nodule growth. The calibration of alfalfa tissue composition was initiated from soybean composition analogy but was improved with values from alfalfa literature. There was considerable iteration in optimizing parameters for the processes outlined above where comparisons were made to measured data. After adaptation, the Root Mean Square Error and d-statistic of harvested herbage averaged across 58 harvests (yield range: 990–4617 kg ha^{-1}) were 760 kg ha^{-1} and 0.75, respectively. In addition, good agreement was observed for Leaf Area Index (LAI) (LAI range: 0.1–6.7) with d-statistic of 0.71. Simulated belowground mass was within the range of literature values. The results of this study showed that CROPGRO-PFM-Alfalfa can be used to simulate alfalfa growth and development. Further testing with more extensive datasets is needed to improve model robustness.

Core Ideas

- Alfalfa is the main forage legume in crop livestock systems worldwide.
- There is still a scarcity of perennial crop models for alfalfa simulation.
- Regrowth and herbage yield depend on reserves, seasonal temperature and daylength.
- A systematic procedure was followed to develop species and cultivar parameters.
- CROPGRO-PFM-alfalfa is available in the latest DSSAT model version (4.7).

Published in Agron. J. 110:1777–1790 (2018)
doi:10.2134/agronj2017.12.0680
Available freely online through the author-supported open access option

Alfalfa (*Medicago sativa* L.) is the main forage legume in crop livestock systems worldwide, with the greatest amount of feed proteins per unit area among the forage and grain legumes (Huyghe, 2003). Changes in forage yield and nutritive value due to climate change are likely to affect the agronomic, economic, and environmental performance of dairy farms. It has been estimated that two-thirds of the potential yield of major crops is usually lost due to adverse growing environments (Bajaj et al., 1999). Accurate prediction of alfalfa yield and growth stages is important in scheduling management practices such as sowing dates, pesticide applications, irrigation scheduling, and cutting frequency or grazing. Timely management can greatly increase the quantity and quality of harvested alfalfa (Sanderson et al., 1989). Crop models can be useful tools for management and decision making in crop production systems by attempting to schedule critical growth stages during the most favorable environmental conditions (Charles-Edwards et al., 1986). Furthermore, computer simulation models after calibration and validation with experimental data provide yield prediction and allow for studying the influence of management strategies and environmental factors on crop growth and development without conducting costly field experiments (Barnes et al., 1988). When physiological processes are well understood, they can be synthesized with crop models, which then become important tools in research by assisting decisions in breeding programs and for soil and crop management, as well as being useful in future climate change assessment (Asseng et al., 2013).

Over the past few decades, several simulation models have been specifically developed for alfalfa. The first alfalfa model SIMED (Holt et al., 1975; Schreiber et al., 1978) is a crop growth model that takes into account dry matter partitioning among leaves, stems and roots. It incorporated most physiological processes but not the regrowth process after cuttings and does not include nonstructural carbohydrates. The second alfalfa model developed was ALSIM (Fick, 1981) which had

W. Malik, F. Dechmi, Agrifood Research and Technology Centre of Aragon (CITA), Soil and Irrigation Dep. (EEAD-CSIC Associated Unit), Avda. Montañana 930, 50059 Zaragoza, Spain; K.J. Boote, Dep. of Agricultural and Biological Engineering, Univ. of Florida, Gainesville, FL 32611; G. Hoogenboom, Institute for Sustainable Food Systems, Univ. of Florida, Gainesville FL 32608; J. Cavero, Dep. of Soil and Water, Estación Experimental de Aula Dei (CSIC), Avda. Montañana 1005, 50059 Zaragoza, Spain. Received 1 Dec. 2017. Accepted 26 Apr. 2018. *Corresponding author (wmalik@cita-aragon.es).

Abbreviations: CP, crude protein; DM, dry matter; LAI, leaf area index; N_2, dinitrogen; RMSE, root mean square error; SLA, specific leaf area; SLW, specific leaf weight; TB, base temperature; TM, maximum (failure) temperature; TO1, first optimum temperature; TO2, second optimum temperature.

subroutines to handle buds for regrowth after a cutting. The model ALSIM 1 (level 1) was developed using monthly average air temperature and solar radiation data for just the growing season, and assumes no limitation on alfalfa production from soil water supply or soil fertility. Thus, the model prediction of yield represents the potential rather than the actual yield. The ALFALFA 1.4 model by Denison and Loomis (1989) was a physiological-based alfalfa model that simulates alfalfa growth and development beginning with tissue and organ-level information, and then growing leaf and stem including internodes and underground structures (crown, taproot, and fibrous roots). The model ALF2LP (Bourgeois, 1990), an offshoot of ALSIM, considers the effects of total nonstructural carbohydrate reserves for the spring restart; it also simulates daily biomass increments of different components of the plant (leaves, stems, basal buds) and considers alfalfa forage; moreover, it considers the age of the crop as a limiting factor on radiation use efficiency. Jégo et al. (2015) demonstrated the ability of the Integrated Farm System Model (IFSM) to accurately predict the forage yield and neutral detergent fiber concentration of each harvest cutting within the growing season of a timothy-alfalfa mixture. One of the assumptions of the IFSM model is that the soil is well drained with no significant fertility limitations, which may tend to overestimate average yield. Leaf mass, stem mass, and leaf area are set to zero after each harvest, which is not appropriate for forages (Rotz et al., 2012). The STICS model is a generic crop model, based on radiation use efficiency, with features that allow the simulation of several aspects of crop production. However, because some processes (e.g., ammonium volatilization, drought resistance, etc.) are not taken into account, the use of STICS is presently limited to several cropping systems (Brisson et al., 1998). CropSyst (Stöckle and Nelson, 1999; Stöckle et al., 2003) is a deterministic, process-based, daily time-step cropping systems simulation model that was adapted to simulate the growth of Italian ryegrass (Confalonieri et al., 2001) and alfalfa (Confalonieri and Bechini, 2004) in rotation schemes with corn for silage production. The authors reported good results, although they point out some limitations, such as the absence of defoliation schedules and reserve remobilization during regrowth. Moreover, CropSyst does not explicitly simulate the role of crown and roots for regrowth after dormancy and after cutting harvests. Therefore, while there are few simulation models for alfalfa available, they are focused primarily on potential production and have limitations in simulating crop physiological and morphological aspects.

A physiologically-based crop model (CROPGRO) (Boote et al., 1998; Jones et al., 2003) was originally developed for grain legumes and is widely used. It is one of the primary crop models along with the CERES cereal models (Ritchie and Otter, 1985) in the Decision Support System for Agrotechnology Transfer (DSSAT) software package (Hoogenboom et al., 2015). The CROPGRO model uses a modular approach, which allows introducing a new crop by modifying values in a species crop template file without changing any computer source code (Boote et al., 1998; Jones et al., 2003). It has been modified for several annual legumes such as faba bean (Boote et al., 2002), velvet bean (Hartkamp et al., 2002), chickpea (Singh and Virmani, 1996), and pigeonpea (Alderman et al., 2015). Furthermore, CSM-CROPGRO-PFM is a modified-coded perennial version of CROPGRO that has been adapted to simulate agronomic responses of several perennial pasture species such as *Paspalum notatum* Flüegge (Rymph et al., 2004), *Brachiaria brizantha* Stapf (Pedreira et al., 2011; Pequeno et al., 2014), and *Panicum maximum* Jacq. (Lara et al., 2012). Adapting an existing mechanistic model such as CROPGRO-PFM has advantages because many processes are similar across species and well simulated which allows taking advantage of the modular subroutines in CROPGRO that simulate soil water balance, soil N balance, soil organic matter–residue dynamics, pest and disease damage, and other processes. The model CROPGRO-PFM includes more detailed description of plant phenology, reserve compound utilization, growth of reserve organs, and regrowth initiation after defoliation (stubble mass and leaf proportion) which are important aspects for forages (Rymph et al., 2004). Using CROPGRO allows to capture greater physiological detail of leaf-level photosynthesis coupled to hedge-row photosynthesis, explicit nodule growth and N_2 fixation, plant uptake of N from the soil, growth and maintenance respiration and internal plant carbohydrate. In addition, adaptation of CROPGRO will allow to use the weather handling, risk management assessment, and GIS–spatial programs and to take advantage of the standard input–output file conventions of the DSSAT models (Boote et al., 2002).

However, despite alfalfa's importance for livestock feeding around the world, an alfalfa growth and yield simulation model is not included in the DSSAT software package. The objectives of the present work are (i) to adapt the CROPGRO-PFM model to simulate the growth and yield of alfalfa, and (ii) to describe the process of adapting the model based on creation of a species file and cultivar traits for this new forage species in DSSAT.

MATERIALS AND METHODS

Field Experiment Data

Six experimental data sets used for model adaptation reflected eight harvest years and came from 18 × 18 m plots irrigated with a sprinkler irrigation system located in the Ebro valley (Northeast Spain). Four experiments were performed in farmer fields at Almudévar irrigation district (42°02′ N, 0°34′ W, 456 m above sea level.) and two were conducted at the experimental farm of the Agricultural Research Service of Aragón in Montañana (41°44′ N, 0°49′ W; 222 m above sea level). At the Almudévar site, two fields were sown on 20 Sept. 2015 (Exp. 1 and 2) and two fields were sown on 1 July 2016 (Exp. 3 and 4). The fifth experiment was sown in Montañana on 14 Apr. 2013 (Exp.5). The last included experiment (Exp.6) was conducted in Montañana over 3 yr (2012, 2013, and 2014) and is described by Cavero et al. (2017). Sowing density ranged from 350 to 400 seeds m^{-2}. The cultivar ecotype (*Aragón*) was grown in all six experiments, and is characterized by group dormancy of 7, violet flowers, medium precocity, and very good regrowth capacity after harvest (Maynar, 1986). All experiments are characterized by Mediterranean semiarid climate, with annual average maximum and minimum daily air temperatures of 21 and 7°C in Almudévar and 21 and 8°C respectively in Montañana. The annual average precipitation is 324 mm and 326 mm and the annual average grass reference evapotranspiration (ET_0) is 1227 mm and 1216 mm in Almudévar and Montañana, respectively. Meteorological data for the study period are summarized in Table 1. For each experimental plot, soil sampling was performed to determine the main soil physical characteristics and soil initial

Table 1. Monthly average meteorological data observed during the evaluation period at the experimental sites in Almudévar and Montañana, Spain.

Weather variable	Jan.	Feb.	Mar.	Apr.	May	June	July	Aug.	Sept.	Oct.	Nov.	Dec.
						Almudévar 2015–2017						
Max. temperature (°C)	11	12	16	20	24	30	34	32	26.5	21	14	10
Min. temperature (°C)	0.4	1	3	5	9	13	16	15	12	8	5	1
Solar radiation (MJ $m^{-2}d^{-1}$)	7	11	15	22	25	28	27	24	19	13	7	5
Rainfall (mm)	18	47	60	20	15	9	23	35	14	23	58	3
ET_0† (mm)	34	44	81	111	153	184	208	180	117	67	34	14
						Montañana 2012–2017						
Max. temperature (°C)	13	16	20	22	28	33	32	29	24	17	11	12
Min. temperature (°C)	2	3	6	8	12	16	16	14	11	7	3	2
Solar radiation (MJ $m^{-2}d^{-1}$)	9	14	19	22	26	27	25	19	13	8	5	7
Rainfall (mm)	34	28	28	26	16	19	11	15	17	46	7	18
ET_0† (mm)	49	65	90	114	137	162	140	96	59	30	18	28

† ET_0: Reference evapotranspiration calculated according to the FAO Penman–Monteith method, mm d^{-1}

conditions for model inputs (Table 2). For all experiments, soil field capacity was considered as initial soil water content. The soil root growth factor (SRGF) is the relative root length distribution factor (0.00–1.00) in respective soil layers that defines the shape of the potential root length density with soil depth, which was calculated by SBUILD program included in DSSAT model based on input of measured soil characteristics (layer thickness and depth, clay, silt, coarse, and organic carbon fractions).

Daily meteorological data were recorded by automatic weather stations (Campbell Scientific, Logan, UT) located near the experimental plots in each location. For Exp. 1, 2, 3, and 4, crop management data were collected from the farmer using a survey at the end of the year such as tillage practices, fertilization amounts and timing, irrigation management (doses and schedule). Leaf area index was measured weekly in each plot using a model LAI 2000 plant canopy analyzer (LI-COR, Lincoln, NE) from May 2016 to May 2017.

All tillage operations were made with commercial equipment. Five to six alfalfa harvests were performed at each experimental field each year. A commercial cutting machine 3-m wide was used to cut the alfalfa. In experiments 1 to 5, a sample of 1 m^2 was randomly selected and forage biomass was manually harvested before machine cutting to quantify forage yield at each harvest period. In experiment 6, alfalfa was allowed to dry for 1 day in the field and then the forage was weighed from each experimental plot from two samples (2 × 6 m). The alfalfa forage of each sample was weighed and a subsample was taken and dried at 60°C to determine the moisture content. Once dried, the subsample was ground and analyzed to determine the N content by combustion (TruSpec CN, LECO, St. Joseph, MI). Then, to estimate crude protein (CP), the N percentage was multiplied by conversion factor equal to 6.25 (FAO, 2003). The remaining alfalfa was left in the field for sun drying after cutting during 3 day and then removed and transported to a dehydration plant.

Approach for Model Adaptation

To adapt CROPGRO-PFM for alfalfa, two approaches were followed to develop the required species file and cultivar traits based on (i) values and relationships reported from the literature and inverse modeling techniques and (ii) a Bayesian optimization approach to compare simulated and measured experimental growth analysis data on alfalfa in the Ebro valley (Northeast Spain).

Table 2. Soil profile characteristics for the experimental fields in Almudévar (Exp. 1, 2, 3, and 4) and Montañana (Exp. 5 and 6).

Depth	Clay	Silt	OC†	LL	DUL	SAT	BD	SRGF
cm		%			v/v		g cm^{-3}	
Exp. 1								
30	43	51	1.8	0.117	0.433	0.497	1.6	1
60	6	70	0.5	0.22	0.449	0.553	1.5	0.407
90	24	60	0.8	0.219	0.470	0.507	1.5	0.223
120	6	67	0.4	0.223	0.464	0.546	1.4	0.122
Exp. 2								
30	38	54	1.4	0.225	0.439	0.497	1.6	1
60	26	58	0.6	0.243	0.407	0.553	1.5	0.407
90	12	64	0.2	0.278	0.389	0.507	1.5	0.223
120	9	60	0.2	0.268	0.373	0.546	1.4	0.122
Exp. 3								
30	47	31	1.7	0.246	0.412	0.443	1.6	1
60	47	34	1.2	0.205	0.334	0.425	1.4	0.407
90	38	28	0.9	0.156	0.286	0.425	1.2	0.223
120	36	21		0.156	0.266	0.418	1.2	0.122
Exp. 4								
30	31	51	1.5	0.136	0.359	0.512	1.3	1
60	32	54	1	0.214	0.369	0.484	1.3	0.47
90	36	54	1.1	0.224	0.528	0.572	1.3	0.223
120	37	55	0.9	0.235	0.292	0.468	1.3	0.122
Exp. 5								
30	13	50	0.7	0.111	0.244	0.497	1.5	1
60	11	55	0.2	0.086	0.218	0.553	1.5	0.607
90	12	54	0.2	0.083	0.218	0.507	1.5	0.423
120	11	46	0.2	0.086	0.237	0.546	1.4	0.322
Exp. 6								
30	51	28	1.04	0.174	0.338	0.497	1.5	1
60	50	31	0.71	0.19	0.35	0.453	1.5	0.407
90	55	31	0.54	0.189	0.356	0.407	1.5	0.223
120	53	33	0.48	0.199	0.362	0.446	1.4	0.122
160	53	30	0.45	0.185	0.348	0.450	1.32	0.061

† OC, organic carbon; LL, lower limit; DUL, drained upper limit; BD, bulk density; SAT, saturated water content; SRGF, soil root growth factor.

The DSSAT-CSM version 4.6 was used for this study (Hoogenboom et al., 2015). The CSM-CROPGRO–PFM (hereafter, called CROPGRO) parameterized for *Bracharia brizantha* cv. Marandu (Pequeno et al., 2014) was used as a starting point for alfalfa adaptation. A characteristic specific to the forage model is the MOW input file, which is used to define

the harvest dates, the amount of live aboveground mass remaining (MOW = live stubble mass), percentage leaf of the stubble (RSPLF), and a "re-staged" leaf number (MVS) at the time of top growth harvest. The MOW value, which characterizes the non-harvested mass that remains in the field, was set at 1000 kg ha^{-1} (hypothetical mass) because actual stubble mass in the field had not been measured. Wiersma and Wiederholt, (2007) reported about 1100 kg ha^{-1} for every 2.5 cm in stubble height which is consistent with our estimated value and stubble height. The MVS parameter and the RSPLF (hypothetical number and percentage) in the MOW file were set at 2 and 20%, respectively.

The Penman–Monteith FAO 56 method was used in our study to calculate potential ET because, according to Saseendran et al. (2008), the Priestley and Taylor method tends to overpredict ET slightly in cooler but relatively arid locations. The CENTURY model converted to daily step and linked to DSSAT models by Gijsman et al. (2002) was used as it is more flexible than the CERES Godwin module in handling different agricultural systems including decomposition of plant litter deposited to the surface during the growing season and root–rhizome–stolon mass that senesces in the soil during the long, multi-year growth of perennial crops. Leaf photosynthesis mode was simulated in the model, meaning that hourly leaf photosynthesis is simulated and scaled up to hourly and then daily canopy assimilation, based on the sunlit and shaded leaf area approach (Boote and Pickering, 1994).

A systematic adaptation procedure of Boote et al. (2002) was followed. First, the cardinal temperature parameters and critical leaf N concentrations driving leaf photosynthesis were based on sensitivity analysis and the literature. Second, where values of alfalfa tissue composition were lacking in the literature, composition of soybean organs was used. Third, partitioning to leaf, stem, taproot, and fibrous root during the seedling phase and perennial phase were modified by comparing simulated and measured total biomass and leaf area during the harvest seasons, along with simulation of reasonable taproot and fibrous root similar to published values (Teixeira et al., 2007; Meuriot et al., 2004). Fourth, nodule growth, dinitrogen (N_2) fixation parameters were calibrated based on sensitivity analysis and an iterative inverse modeling process. Fifth, a Bayesian optimizer was used to optimize temperature parameters for photosynthesis and daylength-dependent parameter effects on partitioning. There was considerable iteration of the steps outlined above where always comparisons were made to measured data (herbage, leaf area index, herbage CP, and plant N concentration).

Optimization Method and Statistics for Evaluating Model Performance

When field observations or reported values for parameters in the literature were missing, an optimization process was used, seeking for the best fit of model simulation to observed variables (such as measured yield) that were influenced by these parameters. This process is called inverse modeling and was performed either by changing parameter values manually, until a value is reached that achieves simulations near to observations, or by using a parameter estimation tool based on Bayesian optimizer. Alderman et al. (2015) previously used this Bayesian optimization tool to adapt the CROPGRO model for pigeonpea. The Bayesian optimizer is a hybrid algorithm program incorporating a Gibbs sampler (Casella and George, 1992) within a version of the Metropolis–Hastings algorithm (Chib and Greenberg, 1995). Essentially, the algorithm consists of generating vectors of candidate parameter values and evaluating them with the following log-likelihood Eq. [1].

$$\ln\left(L\left(\Theta_k|x\right)\right)=\sum_{i=1}^{N}-\ln\frac{1}{\sigma_i}-\frac{\left(x_i-\hat{x}_i\right)^2}{2\sigma_i^{\,2}} \quad [1]$$

where Θ_k is the k^{th} vector of parameter values, x_i is the i^{th} observation from a vector of N observations, $\hat{x}_i$ is the model predicted value using Θ_k that corresponds to x_i, and σ_i is the standard deviation of the sample for x_i. We took into account knowledge of how a given parameter drives the model performance of a given model output variable and whether the resulting parameter fell within the range of values (minimum to maximum) reported in the literature or from previous knowledge.

For evaluating model performance after optimization or adaptation, we used the observed/simulated ratio, root mean square error (RMSE; Eq. [2]) and the Willmott agreement index (d-statistic; Eq. [3]) (Willmott, 1981; Willmott et al., 1985).

$$RMSE=\sqrt{\frac{1}{N}\sum_{i=1}^{N}\left(Y_i-\hat{Y}_i\right)^2} \quad [2]$$

Where N is the total number of data points for comparison, Y_i is a given observed value, and $\hat{Y}_i$ is the corresponding value predicted by the model. A better model prediction will produce a smaller RMSE. The Willmott agreement index is given by

$$d=1-\left[\frac{\sum_{i=1}^{N}\left(Y_i-\hat{Y}_i\right)^2}{\sum_{i=1}^{N}\left(\left|\hat{Y}_i-\overline{Y}\right|+\left|Y_i-\overline{Y}\right|\right)^2}\right],\ 0\le d\le 1 \quad [3]$$

Where N is the number of observed data points, Y_i is a given observed value, $\hat{Y}_i$ is the corresponding value predicted by the model, and $\overline{Y}$ is the mean of the observed data. A d index near to 1 indicates good model prediction. The crop model parameters used in this paper are typical of physiological models such as CROPGRO and the associated evaluation statistics are widely used in model calibration and validation studies in crop modeling (Lara et al.,2012; Pequeno et al., 2014).

RESULTS AND DISCUSSION

The results presented in Figures and Tables show simulations of final adaptations, and the following text describes the how and why of parameter adjustments that were made. Because the starting point of the model was a tropical C_4 grass (brachiaria), many of the modifications were associated with modified (lower) cardinal and optimum temperatures for all important processes as well as modified compositions typical of a C_3 legume such as alfalfa.

Model Adaptation

Cardinal Temperatures for Development Rate and Growth

The phenology in the CROPGRO model is driven by a set of cardinal temperature (°C) parameters: base temperature (TB), first optimum (TO1), second optimum (TO2), and maximum

Table 3. Model parameter names, definitions, initial brachiaria values (Pequeno et al., 2014), and calibrated alfalfa values for photosynthesis, phenology, growth, and senescence parameters.

	Definition	Initial brachiaria	Calibrated alfalfa
FNPGN (4)	Minimum and critical leaf N concentration for parabolic function that reduces photosynthesis due to low leaf N concentration (% units).	0.80 4.00	1.90 5.50
XLMAXT(2,3)	Base temperature and optimum temperature for hourly temperature effect on light- and CO_2-saturated electron transport of photosynthesis.	6.2 40.2	0.2 33.0
YLMAXT(2,3)	Relative effect of temperature on rate of electron transport corresponding to given temperature (XLMAXT).	0.0 1.0	0.0 1.0
FNPGL(1,2)	Describes relative effect of minimum night temperature (TMIN) on next day's single leaf light-saturated photosynthesis rate. 2-point parabola (QDR)	5.1 22.2	–5.1 8.2
PGEFF	Quantum efficiency of leaf photosynthesis, defined at 350 ppm CO_2, 21% oxygen, and 30 °C. Set from published values in literature, Ehleringer and Bjorkman, (1977).	0.0650	0.0541
SLWREF	Specific leaf weight at which LFMAX is defined (g cm^{-2}).	0.0071	0.0026
SLAREF	The specific leaf area (cm^2 g^{-1}) of the standard reference cultivar at peak early vegetative phase, under optimum temperature, water, and light.	190	280
PGREF	Reference value for leaf photosynthesis, used in daily canopy light response curve (mg CO_2 m^{-2} s^{-1}).	1.8	1.4
SLAMAX	The (thinnest) leaves can be under low light cm^2 g^{-1}.	340	460
SLAMIN	The (thickest) leaves can be under high light cm^2 g^{-1}.	139	250
FINREF	The specific leaf area (cm^2 g^{-1}) of leaves at plant emergence, scaled via SLAVAR though.	150	180
TURSLA	Modifier of water stress (TURFAC) effect on leaf area expansión.	1.2	1.5
FREEZ1	Temperature thresholds for tissue loss due to freezing.	0	–2
TB, TO1, TO2, TM for vegetative development	Base temperature (TB), first optimum (TO1), second optimum (TO2), maximum temperature (TM) for vegetative development (°C).	11.1 30.2 40 45	3 25 33 45
TB, TO1, TO2, TM for reproductive development	Base temperature (TB), first optimum (TO1), second optimum (TO2), maximum temperature (TM) for reproductive development (°C).	12 28 33 45	4 28 33 45
LFMAX	Maximum leaf photosynthesis rate at 30 C, 350 vpm CO2, and high light (mg CO_2 m^{-2} s^{-1}).	1.8	1.4
SLAVR	Specific leaf area of cultivar under standard growth conditions (cm^2g^{-1}).	190	280
RDRMT	Relative dormancy sensitivity, daylength effect on partitioning.	0.475	0. 421

temperature (TM), defined for rate of leaf appearance and both early and late reproductive development. Since the forages remain vegetative most of the time, calibration of the cardinal temperature was focused primarily on the vegetative development for which the TB, TO1, TO2, and TM were set to 3, 25, 33, and 45°C, respectively as summarized in Table 3. The cardinal temperatures for reproductive stages were maintained similar to the vegetative phase except for TB for the early reproductive development (affects time to flower) which was set to 4°C. Several sources were used to document TB for vegetative development and most alfalfa growth models consider 5°C for accumulated growing degree days during all growth stages (Onstad and Fick, 1983; Fick et al., 1988; Confalonieri and Bechini, 2004; Wolf and Blaser, 1971; Sharratt et al., 1989). However, Jeney (1972) reported a lower value of 0°C for calculation of accumulated thermal time until alfalfa flowering. Thus, the calibrated cardinal temperatures for development were within the range of values reported in the literature.

The temperature parameters for photosynthesis and leaf area growth were evaluated against observed biomass accumulation data, which spanned growth over the full annual seasonal cycle. Thus, this method allows the setting of the temperature-dependencies of the photosynthesis and leaf growth processes, especially for the TB. Zaka et al. (2016) analyzed a series of experiments at seven growth temperatures between 5 and 35°C using four cultivars from temperate and Mediterranean regions and reported that 25 to 35°C were the TO1 and TO2 respectively within which the net assimilation rate in standard condition was at its maximum. Bula (1972), obtained the highest biomass yields at 25°C for three alfalfa cultivars, but one cultivar performed well in the range 20 to 30°C. Gowgani (1977), obtained the highest daily biomass at first flowering when a 20/10°C (day/night) regime was used. However, most of these manuscripts dealt with a few cultivars in different locations from the study area. Therefore, we believe that the genetic origin of the cultivar may influence the optimal temperature chosen as a model parameter.

The specific leaf area (SLAVR) of a cultivar under optimum growth condition was set to 280 cm^2 g^{-1} as a standard reference cultivar at peak early vegetative growth, under standard growing conditions (optimum temperature, water, and high light). The modified value for SLA is consistent with the values (265 cm^2 g^{-1}) for ALSIM model reported by Bourgeois (1990) and that measured (282 cm^2 g^{-1}) by Antolín et al. (1995) for

well-watered N-fixing alfalfa plants. Confalonieri and Bechini (2004) used a calibrated value of 260 $cm^2\ g^{-1}$ for the CropSys model. Other measured values reported in the literature are 303 $cm^2\ g^{-1}$ (average of the first two sampling dates after cutting (Sheehy and Popple, 1981), and 227 $cm^2\ g^{-1}$ (Buntin and Pedigo, 1985) for rainfed alfalfa plants although water deficit is known to reduce SLA.

There are two parameters that together result in the value of 280 $cm^2\ g^{-1}$ for SLA, SLAMAX and SLAMIN, which define the thinnest and thickest leaves under very low and high light, respectively (500 and 250 $cm^2\ g^{-1}$, respectively). In addition, there are programmed temperature effects (also via the species file) that reduce SLA from its optimum under cold or too hot temperatures, which were calibrated against SLA data throughout the annual cycles. Considering the simulation of all six experiments, the SLA ranged throughout the year between 150 and 330 $cm^2\ g^{-1}$ which fit within values reported in the literature. The estimated mean SLA by the model after setting these parameters was 235 $cm^2\ g^{-1}$, which confirm a consistent set of the parameters that control SLA.

Photosynthesis Parameters

Alfalfa falls into the group of C_3 photosynthesis pathway that has a photosynthetic capacity and photosynthetic efficiency lower than most tropical grasses (Brown and Gracen, 1972; Kajala et al., 2011). Based on that concept and other references on the literature, the maximum leaf photosynthesis (LFMAX) in the CUL file was reduced from 1.8 (initial value used for C_4 forages) to 1.40 mg $CO_2\ m^{-2}\ s^{-1}$ for alfalfa (C_3 plant). In fact, alfalfa contains ribulose–1,5diphosphate carboxylase as the main carboxylation enzyme in CO_2 fixation (Huffaker et al., 1970), rather than phosphoenolpyruvate carboxylase, which is mainly responsible for CO_2 fixation in tropical grasses and a few dicots (Hatch and Slack, 1966, 1967). Boller and Heichel (1984), compared effective to ineffective nodule type cultivars of alfalfa for leaf photosynthetic rate during vegetative and early flowering stage, and observed that the leaf photosynthesis rate ranged between 1.06 and 1.72 mg $CO_2\ m^{-2}$ leaf s^{-1}. Other values of LFMAX from the literature were reported by Osment (1978) who found differences in photosynthetic rates among 30 studied alfalfa clones (1.59–0.30 mg $CO_2\ m^{-2}\ s^{-1}$). Pearce et al. (1969) found that some cultivars differed in photosynthetic capacity as much as 33%. These differences were associated with specific leaf weight (leaves with high specific weight had higher photosynthesis rates). Maximum rate of CO_2 uptake by young leaves vary from 20 to almost 70 mg $dm^{-2}\ h^{-1}$ (0.55–1.9 mg $CO_2\ m^{-2}\ s^{-1}$) (Murata et al., 1965; Wolf and Blaser, 1972). Much of this wide range of photosynthetic capacity is attributed to variation in genotype and environmental conditions during growth and measurement. The specific leaf weight (SLWREF) at which LFMAX is defined was set to 0.0026 g cm^{-2}, and the model varies the actual rate as a function of SLW, using the concept of strong dependence of LFMAX on SLW similar to that found by Pearce et al. (1968) in which photosynthesis increased from 20 ± 7 to 50 ± 8 mg $CO_2\ dm^{-2}\ h^{-1}$ as SLW increased from 1.9 to 5.3 mg cm^{-2}.

The Bayesian optimizer was used to optimize two temperature parameterization effects on photosynthesis, where the target was the simulated versus observed herbage mass. First, the sensitivity of single leaf, light-saturated photosynthesis rate to minimum night temperatures (FNPGL) where FNPGL (i) corresponds to night temperature at which the light-saturated leaf photosynthesis of next day is zero, and FNPGL (ii) corresponds to the T_{min} at which there is no effect on next day's photosynthesis, using an asymptotic function. The temperature parameters for FNPGL (1, 2) were set at −5.1 and 8.2°C, respectively. The second optimized parameter is the relative rate of photosynthesis electron transport in response to current hourly temperature for hourly temperature effect on light- and CO_2-saturated electron transport of photosynthesis. This is a 6-point lookup function that describes relative rate of photosynthetic electron-transport (YLMAXT) in response to temperature (XLMAXT). Changes were made to set base and optimum temperature XLMAXT (2, 3) at 0.2 and 33°C, respectively, which correspond to YLMAXT (2, 3) of 0.0 and 1.0, respectively (Table 3).

Nitrogen is a crucial component of photosynthetic enzymes; its effect on photosynthesis is accounted for using a one-sided parabolic curve and the parameters FNPGN 1 and 2 are the leaf N concentrations for zero and maximum photosynthesis rates, respectively (Pequeno et al., 2014). The leaf N concentration effect on photosynthesis (FNPGN) is given in Table 3. We consider that alfalfa and soybean have a similar pattern and sensitivity of photosynthesis to leaf N concentration. The amount of photosynthetic enzymes in the leaf affects photosynthetic rate as well. Generally, higher N concentrations in the leaves are correlated with higher levels of these enzymes and higher photosynthetic capacity. The PGEFF–Quantum efficiency of leaf photosynthesis, defined at 350 ppm CO_2, 21% oxygen, and 30°C is 0.0541 (same as CROPGRO–soybean value), a value consistent for all C_3 crops that was taken from Ehleringer and Bjorkman (1977).

Dry Matter Partitioning

During vegetative growth, all assimilate is allocated to vegetative tissues, with partitioning among leaf, stem, storage (crown–taproot), and root components being dependent on vegetative stage (V-stage) progression (expanded leaf number on main axis). The species file contains an array function that describes the instantaneous daily partitioning among leaf, stem, storage and root tissues, depending on crop developmental stage (vegetative seedling phase and subsequently the perennial phase). These are look up functions with linear interpolation that relate actual plant V-stage (number of nodes on stem) to partitioning coefficients. XLEAF is an array of values of seedling V-stages, used for all plant organs, and YLEAF, YSTEM, and YSTOR are the equivalent seedling partitioning coefficients, respectively, for leaf, stem, and storage organs. Using the same logic, XLFEST is the V-stage scale for established perennial partitioning, and YLFEST, YSTEST, and YSREST are the correspondent partitioning coefficients. First, the model will use the seedling partitioning if the plant is still in the juvenile phase which lasts up to 60 photothermal days (SDLEST = 60) after emergence. After that point, the model switches to the established partitioning set, which allows differential patterns of partitioning as a function of successive main stem node number (V-stage), but which V-stage is re-set to MVS after each harvest. As there were no literature values for partitioning of dry matter to organs at different vegetative stages of growth, the partitioning of brachiaria (Pequeno et al., 2014) was used as a starting point. However, the performed simulations showed the need to adjust the partitioning

parameters for alfalfa. The first modification consisted of an increase in allocation to leaf and stem growth in the seedling phase, while allocating less to storage organ growth (because alfalfa prioritizes partitioning to leaf during its initial seedling growth phase) (Thiébeau et al., 2011; Teixeira et al., 2009). Figure 1 illustrates the partitioning to all plant organs (leaf, stem, storage organs and roots) during the seedling phase (Fig. 1A) and the established phase (Fig. 1B), where the *x* axis, XLEAF, is a scale of values of V-stages. The partitioning coefficient for roots is obtained by difference, as the sum of partitioning coefficients to all organs must be one (1). The model uses a linear interpolation to compute partitioning change as decimal V-stage progresses. Difficulties in adjusting the partitioning for both phases due to the lack of observed leaf, stem, and root fraction were managed by extrapolating data from literature (Stavarache et al., 2012; Teixeira et al., 2007) and comparing them to the simulated data on leaf percentage, total biomass, roots, and storage (crown–taproot) (Meuriot et al., 2004; Simon et al., 2004).

Leaf Senescence Parameters: Dormancy–Freezing

During the hardening period in winter, the alfalfa plant undergoes biochemical, physiological, and morphological changes that seem to increase its tolerance to freezing temperatures while suppressing aboveground herbage growth (Li et al., 1996). Non-hardened alfalfa cannot survive subzero temperatures, whereas hardened alfalfa is able to withstand temperatures as low as –24°C following development of winter hardiness during the autumn season (Paquin and Lechasseur, 1982). Miller (1994) reported severe yield reduction due to winter injury on 27 to 70% of the alfalfa acreage in Wisconsin and Minnesota during 1989 to 1993. In the CROPGRO-PFM-Alfalfa model, the decrease in forage growth during 'winter' months is adjusted by 'dormancy' parameters, triggered by short photoperiod below which allocation to taproot is increased at the expense of shoot growth, and also dependent on setting of temperature effects that reduce photosynthesis and leaf expansion. In addition, the effect of freezing temperatures is defined by FREEZ1 (set to –2°C), the temperature below which plants lose all leaf tissue. The parameter FREEZ2 (the temperature below which plants including taproot–crown stop to grow completely and start to die) was maintained at –25°C and FRZDC was set at 5% (the rate at which plants die below FREEZ2 temperatures). The adjustment of the FREEZ1 parameter was based on field observations during several winters in our experiments. In addition, the parameter RDRMT modulates the effect of daylength, and can be used to differentiate genotypes that are more or less sensitive to shortening of photoperiod in fall. RDRMT is the relative sensitivity to daylength of the dormancy-related partitioning of a given ecotype (value varying from 0 to 1). A small value of RDRMT (closer to 0) defines an ecotype with less shift in partitioning to storage (taproot) during short daylengths than the standard species ecotype. An RDRMT closer to 1, defines an ecotype exhibiting a greater shift in partitioning during short daylength than the standard species ecotype. This parameter was set at 0.421 by the parameter-estimation algorithm (optimizer). Noquet et al. (2003) reported that a short-day treatment gave lower shoot:root partitioning and resulted in greater vegetative storage protein accumulation in taproots than a long-day treatment and attributed

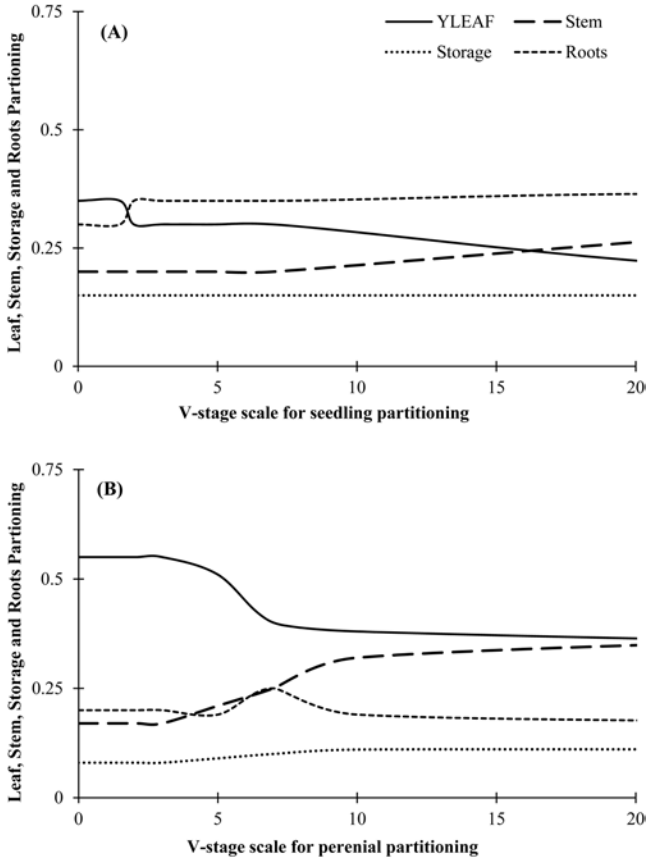

Fig. 1. Instantaneous daily partitioning of dry matter among vegetative components (leaf, stem, storage [taproot–crown], and roots) of alfalfa as a function of V-stage scale for seedling partitioning (A) and perennial establishment (B) after model adaptation.

this to the fact that the leaves and stems are strong N sinks during long days. In addition, the optimizer was successfully used to set the cardinal daylength parameters (FNPTD and FNPMD) at 11.1 and 12.2 h, respectively for relative dormancy sensitivity effect of daylength on mobilization and partitioning to increase seasonal cycling variations during seasonal regrowth. This makes the model sensitive to daylength at daylength less than 12.2 h, reaching a maximum dormancy effect at 11.1 h.

Alfalfa Tissue Composition

The model requires tissue composition to be defined by fractions of six classes of compounds: protein, lipid, lignin, carbohydrate-cellulose, organic acids, and minerals for stem, root, nodule, shell, and seed and storage tissue (Wilkerson et al., 1983; Jones et al., 1989). Growth respiration cost for tissue synthesis is based on the Penning de Vries et al. (1974) approach. The protein composition of new tissue depends on N availability, and there are three cardinal values for protein concentrations: (i) in leaf (PROLFI), stem (PROSTI), root (PRORTI), and storage (PROSRI) for new tissue or tissue grown under luxurious supply of N; (ii) for the minimum concentration for growth (PROLFG, PROSTG, PRORTG, PROSRG); and (iii) for the concentration after remobilization (PROLFF, PROSTF, PRORTF, PROSRF) at which point leaves would abscise, for example. Tissue carbohydrate (including cellulose and C polymers) concentration parameters (PCARLF, PCARST, PCARSH, PCARSD) values were set as the

Table 4. Model tissue composition parameters, definitions, initial (soybean) values and calibrated alfalfa values for composition of leaf, stem, root, seed and taproot.

		Initial values					
	Concentration	Leaf	Stem	Root	Shell	Seed†	Taproot
PRO _ _I	Maximum protein	0.356	0.150	0.092	0.092	0.400	0.250
PCAR_ _	Carbohydrate–cellulose	0.405	0.664	0.711	0.380	0.315	0.711
PLIP_ _	Lipid	0.025	0.020	0.020	0.020	0.050	0.020
PLIG_ _	Lignin	0.070	0.070	0.070	0.280	0.020	0.070
POA_ _	Organic acid	0.050	0.050	0.050	0.040	0.040	0.050
PMIN_ _	Mineral	0.094	0.046	0.057	0.030	0.025	0.057
		Calibrated values					
	Concentration	Leaf	Stem	Root	Shell	Seed[2]	Taproot
PRO _ _I	Maximum protein	0.372	0.194	0.092	0.092	0.400	0.250
PCAR_ _	Carbohydrate–cellulose	0.406	0.555	0.711	0.380	0.315	0.480
PLIP_ _	Lipid	0.022	0.009	0.020	0.020	0.050	0.020
PLIG_ _	Lignin	0.039	0.114	0.070	0.280	0.020	0.070
POA_ _	Organic acid	0.05	0.050	0.050	0.040	0.040	0.050
PMIN_ _	Mineral	0.111	0.048	0.057	0.030	0.025	0.057

† Standard protein concentration of seed.

Table 5. Model parameter names, definitions, initial soybean values and calibrated alfalfa values for nitrogen fixation parameters.

	Definition	Initial values	Calibrated values
NDTHMX-	Maximum nodule death rate, fraction per day.	0.04	0.02
SNACTM	Specific nitrogenase activity of nodule tissues, g N fixed per g of nodule mass per day.	0.05	0.05
FNFXT(4)	Temperature curve (LIN for linear 4-point function) describing specific nitrogenase activity versus soil temperature.	5.0	–2.0
		23.0	15.0
		35.0	30.0
		44.0	44.0
FNNGT(4)	Temperature curve (LIN for linear 4-point function) describing relative nodule growth rate versus soil temperature.	7.0	–1.0
		28.0	19.0
		35.0	30.0
		44.0	44.0

difference between all other tissue composition parameters for a given tissue, thus allowing protein composition to vary dynamically dependent on N stress.

Initially, parameters from the CROPGRO soybean species file were used for setting alfalfa composition tissues due to the close similarity between the two legumes and lacking measured data. Subsequently, some parameters were modified to improve prediction of CP based on literature values (Hintz and Albrecht, 1991; Milić et al., 2011) and by comparison of simulated and measured CP in herbage. For instance, protein concentration in leaf (PROLFI), stem (PROSTI), root (PRORTI), and storage (PROSRI) for tissue grown under luxurious supply of N were based on literature values (Milić et al., 2011; Stavarache et al., 2015). Related tissue parameter modifications are presented in the Table 4. The following parameters such as lipid concentration in leaf (PLIPLF), in stem (PLIPST), mineral concentration in leaf (PMINLF), in stem (PMINST), and lignin in leaf (PLIGLF) and stem (PLIGST), were based on the following references (Fox et al., 1991; Stavarache et al. (2015) and Teixeira et al., 2007).

Nodule Growth and Dinitrogen Fixation

One of the main differences between the simulation of alfalfa and the grasses is the need to simulate N fixation. An important parameterization step was the activation of the nodule growth and N_2 fixation subroutine in CROPGRO code (this was easily done in the source code by specifying the AL crop name as allowing N-fixation. The crop name requirement is needed to prevent someone from turning on N-fixation in the CROPGRO cotton or tomato model, for example). Where feasible, literature values were used for setting parameters, and where information did not exist, sensitivity analyses was used to set relationships to obtain reasonable N_2 fixation rate and nodule growth. For that reason, the temperature sensitivities of these two processes were calibrated in an iterative way by a manual inverse modeling process, to reduce the lags in nodule growth and N-fixation rate that would have unreasonably reduced dry matter growth, either associated with early season cold temperatures or seedling to perennial transition. A similar process had been followed for temperature parameterization of soybean N-fixation (Sexton et al., 1998). For temperature response, we set TB, TO1, TO2, and TM to –1, 19, 30, and 44°C, respectively, for nodule growth (Table 5). Then, for N_2 fixation temperature response, TB, TO1, TO2, and TM were set to –2, 15, 30, and 44°C, respectively. Reports on TB for N_2 fixation range between 2 and 10°C depending on the tropical or temperate origin of the species, while the maximum temperature is for all species between 35 and 40°C (Liu et al., 2011). By contrast, alfalfa is a cool-season tolerant species with relatively low cardinal temperatures. In addition, the NDTHMX (maximum nodule death rate, fraction per day) was reduced from 0.04 to 0.02 to increase the nodule mass and sustain nodule mass into winter-spring seasons. No change was considered for specific nitrogenase activity (SNACTM) value (Table 5).

Table 6. Total biomass, herbage yield, leaf area index (LAI), herbage crude protein (CP), shoot nitrogen concentration (N) and the corresponding statistics averaged over 6 experiments (n = 58 herbage harvests).

	Observed data		Simulated data		Ratio (obs./		
	Mean	Range	Mean	Range	sim.)	RMSE	d-statistic
Total biomass (kg DM ha^{-1})	3889	1706–5617	3751	1983–6434	1.04	728	0.76
Herbage yield (kg DM ha^{-1})	2907	990–4617	2810	1278–5475	1.03	760	0.75
LAI (m^{2}m^{-2})	2.5	0.1–6.7	3.0	0.41–9.6	0.81	2.0	0.71
CP (% of DM)	20.3	16–27	19.9	14–26	1.02	5.2	0.39
N (% of DM)	3.7	2.5–5.5	2.8	1.8–3.7	1.3	1.0	0.3

Evaluation of Adapted Model

Herbage, Total Biomass, and Leaf Area Index

Table 6 summarizes the averages and the range of observed and simulated values of total biomass, herbage yield, LAI, CP, N percentage and the corresponding ratio (Obs./Sim.), RMSE and d-statistic values over the six experiments (n = 58 herbage harvests), after the model adaptation. The observed values of total biomass ranged from 1706 to 5617 kg DM ha^{-1} while the simulated values ranged from 1983 and 6434 kg DM ha^{-1}. Meanwhile the observed herbage yield varied between 990 and 4617 kg DM ha^{-1}, and the simulated herbage yield varied between 1278 and 5475 kg DM ha^{-1}. The low values for both total biomass and herbage correspond to the first cuts during alfalfa seasons. However, the variability of measured herbage (CV = 28%) was slightly higher than that of the simulated (26%).The observed range of values of LAI was 0.1 to 6.7 while the simulated range was from 0.41 to 9.6. The low values of LAI correspond to the early regrowth period and the high values to full vegetative stage (before cutting). The observed herbage CP and N concentration values ranged from 16 to 27% and 2.5 to 5.5%, respectively. The corresponding simulated values ranged from 14 to 26% and from 1.8 to 3.7% for herbage CP and N, respectively. These ranges depend on the timing of harvests and the leaf and stem ratio of the harvested herbage.

In general, good results were obtained for the means of observed and simulated values with a small difference of 138 and 97 kg ha^{-1} for the total biomass (Biomass) and harvested mass (Herbage), respectively (Table 6). Figure 2 shows the relationship between the simulated and observed herbage yields over the six experiments, with a slope of 0.985 (slope of 1.00 is desired) with RMSE of 760 kg ha^{-1}, and d-statistic of 0.75. The RMSE and d-statistic values for biomass were comparable to that for herbage (Table 6). The d-statistic and RMSE for the LAI were 0.71 and 2.00, respectively.

The seasonal growth pattern of the LAI and the total biomass is illustrated in Fig. 3 for Exp 1, which had more observed values for LAI than for biomass. A good agreement was found between observed and simulated values during the growing season for both variables. A high d-statistic of 0.73 and 0.85 was obtained for LAI and total biomass, respectively for Exp 1. The RMSE (nRMSE) of the total biomass and LAI were 625 kg ha^{-1} (14.5%) and 2.15, respectively. The results obtained compare well with other published studies for forage simulations such as for *Panicum máximum* crop where a RMSE (nRMSE) of 478 kg ha $^{-1}$ (7.5%) was obtained and a d-statistic of 0.79 for total biomass (Lara et al., 2012). In addition, Pedreira et al. (2011) obtained a RMSE (nRMSE) of 538 kg ha $^{-1}$ (16%) and a d-statistic of 0.83 simulating the *Brachiaria brizantha*. Pequeno et al. (2014) obtained a RMSE (nRMSE) of 523 kg ha $^{-1}$ (15.5%) and a d-statistic of 0.96

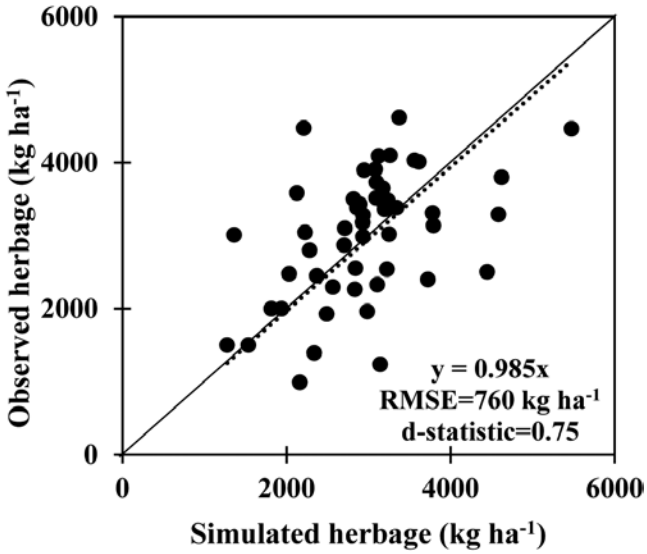

Fig. 2. Simulated and observed alfalfa herbage yields over the six experiments (n = 58) and associated statistics.

simulating the regrowth harvests of *Marandu palisadegrass*. The CROPGRO-Alfalfa model was successful in simulating final and intermediate values of both herbage and LAI.

Tissue Composition

Figure 4 shows the observed and simulated CP of herbage for experiment 6 during three seasons which represents a good number of observations (n = 18). Acceptable results were obtained after the modification of alfalfa composition tissues in the species file. The mean of simulated and observed CP were 18.83 and 18.79 (% of herbage DM), respectively. However, the d-statistic was low (0.16). Conversely, a higher d-statistic than 0.75 was obtained for CP in the two first experiments. Table 6 shows the mean CP averaged over the six experiments with simulated and observed values of 19.9 and 20.3%, respectively. The RMSE was 5.2 (% of herbage DM) and the d-statistic was 0.39.

Dry Matter Partitioning

Observed percent leaf values of harvested herbage were extrapolated from Stavarache et al. (2012) study in Romania for three cuts during the first season, and those values ranged between 42 and 61%. In the study of Simon et al. (2004), the leaf percentage varied between 50 and 53% under different N fertilization and residual leaf area treatments. In our experiments, the simulated percent leaf was around 70% (the average of the 6 experiments). In seedling phase, the first simulated biomass consistently matched the observed dry matter production with a difference of 44 kg ha^{-1} in Exp.1 (Fig. 5), which suggests reasonably good seedling partitioning. During the established phase,

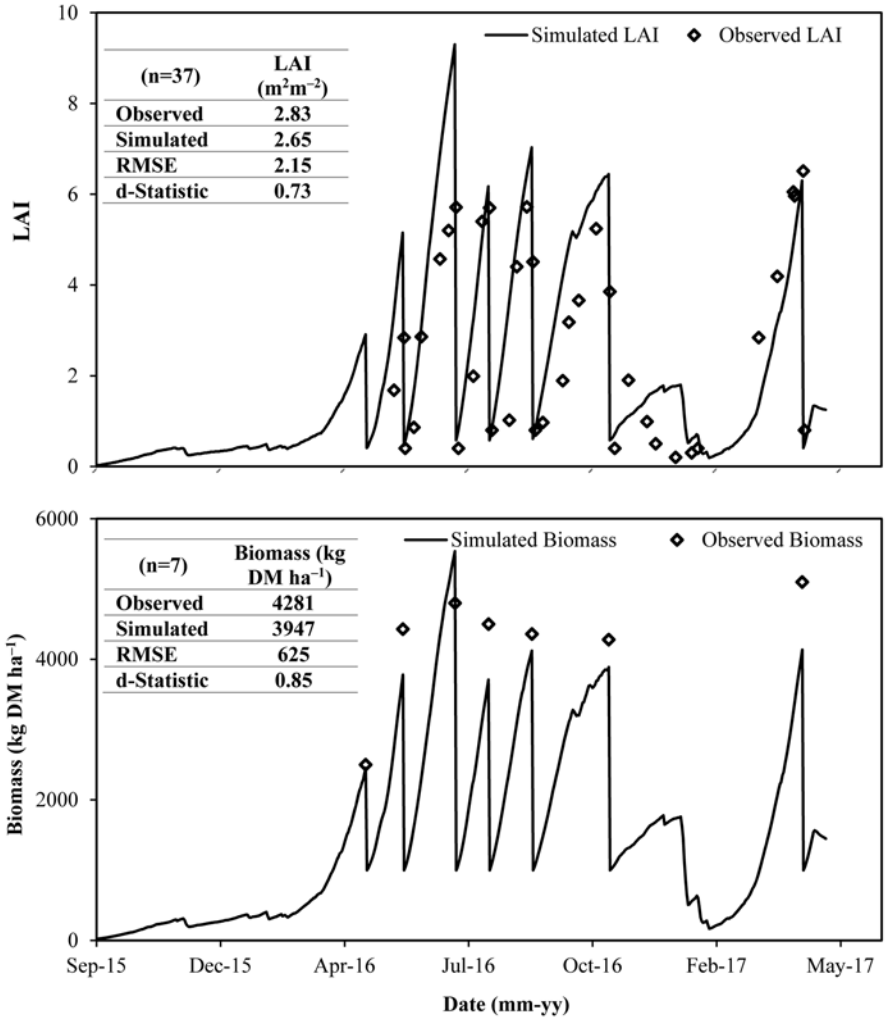

Fig. 3. Comparison of simulated (lines) and observed (symbols) leaf area index (LAI) and biomass over time for Exp. 1 in Almudévar, Spain.

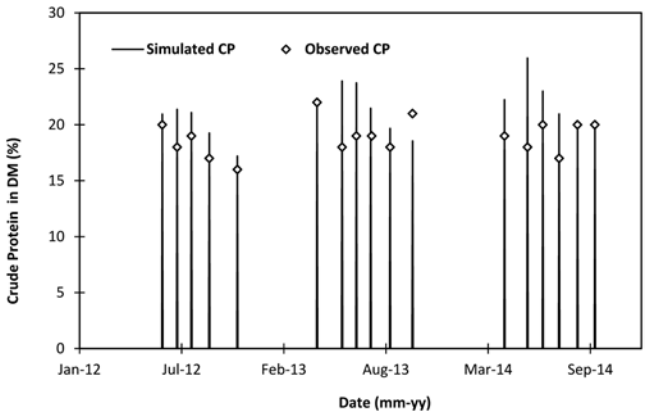

Fig. 4. The observed (dots) and simulated (line) crude protein (CP) as percent of herbage dry matter for Exp. 6 in Montañana, Spain.

our results were consistent with Stavarache et al. (2015) who showed in their experiment of 3 yr in Romanian Forest Steppe that with the advancement of growth stages, from early bud stage until the early bloom stage, the production of stems, leaves and whole plant increased continuously. Regarding the belowground mass, patterns of accumulation and depletion of roots and storage (taproot–crown) of the alfalfa crop were examined during successive four seasons for Exp.5. The simulated fibrous root and storage (taproot–crown) biomass results are within the range of literature values (Fig. 6). Simulations are close to observed data reported by Teixeira et al. (2007), who reported that the sum of crown and taproot DM throughout several cycles ranged from 3.0 to 5.5 t ha^{-1}. The average of the simulated crown and taproot dry matter throughout four seasons in Exp 5 is 3796 kg ha^{-1}, which is within the range of 3000 to 5500 kg ha^{-1} reported by Teixeira et al. (2007). Moot et al. (2015) reported in their study in New Zealand the tendency of dry matter partitioning to the belowground biomass (crown and taproot) was increasing to reach more than 7000 kg ha^{-1} in the fourth growing season. Similar behavior was observed in our simulated experiments where the storage DM was seasonally increasing to a maximum of 5739 kg ha^{-1}. The average of fibrous root for the Exp. 5 over the entire season is 3201 kg ha^{-1}, which is consistent with those reported by Teixeira et al. (2009) and Thiébeau et al. (2011). Meuriot et al. (2004), reported the partitioning of the biomass at the end of alfalfa regrowth (Day 29), with a ratio of herbage vs. taproot of 40% and herbage vs. lateral roots of 45%. The goal was to get simulations to represent values within the range and tendency of literature.

The fibrous root and storage biomass undergo variations during re-growth and winter-dormancy cycles, particularly because of the regrowth phenomena and mobilization of reserves during the regrowth (Teixeira et al., 2009; Volenec et al., 2002). There was a temporal pattern of change in the absolute dry weight of fibrous root with the lowest values of root occurring in spring and

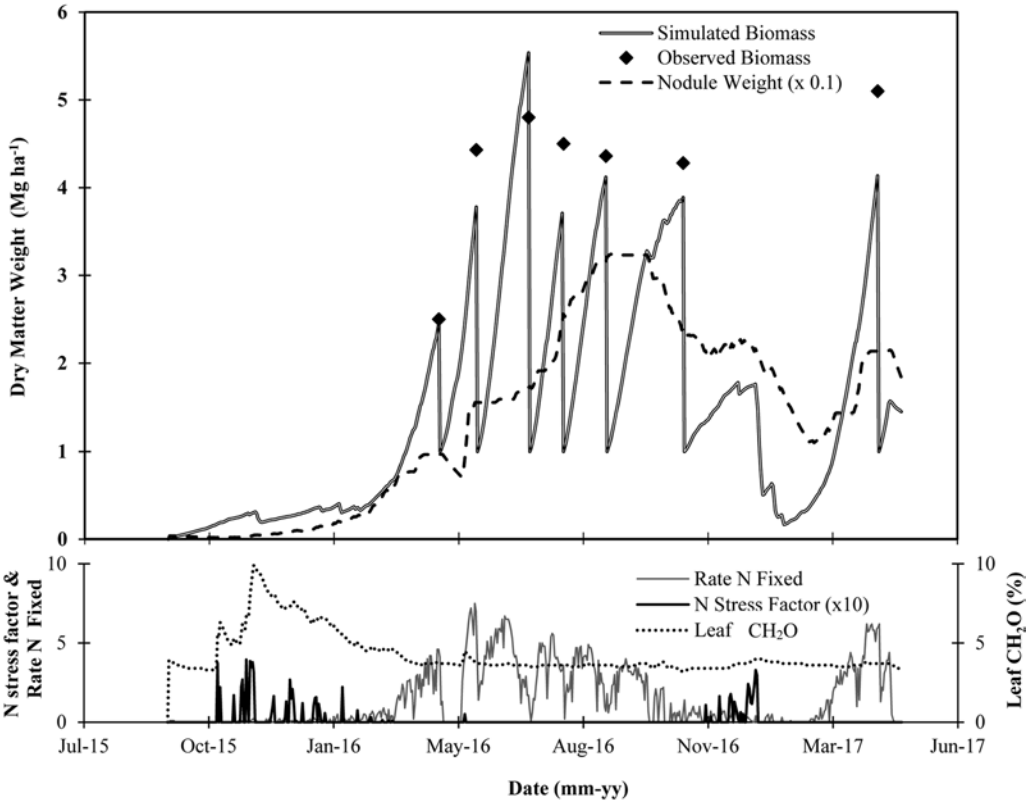

Fig. 5. Simulated leaf nonstructural carbohydrate, N stress factor, rate of N fixation, nodule mass, and observed and simulated biomass over two seasons in Exp.1.

the highest in autumn (Fig. 6). In general, the seasonal patterns indicated that there was a preferential allocation of DM to the perennial organs in late-summer/autumn, regardless of defoliation treatment. The root DM has been observed by Teixeira et al. (2007) to decrease during winter/spring. This decrease is consistent with the idea that root DM decreased due to respiration throughout winter and that some DM is partially remobilized to shoots in early-spring (Avice et al., 2001; Volenec et al., 1996). Observed seasonal differences in root biomass are a function of increasing DM partitioning especially to the taproot component during autumn probably in response to short photoperiods and/or low temperatures (Gosse et al., 1984; Khaiti and Lemaire, 1992).

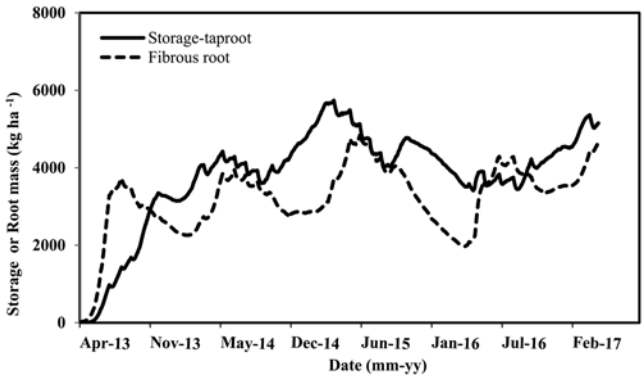

Fig. 6. Seasonal simulation of storage-taproot (solid line) and fibrous root weight (dashed line) over 4 yr for Exp. 5 in Montañana, Spain.

Dinitrogen Fixation and Nodule Growth Pattern

Figure 5 describes the dynamics of nodule growth, N_2 fixation rate, biomass, and nonstructural carbohydrate accumulation during a 2-yr growing period. When simulated N uptake is deficient for growth of new tissues (N stress appears), carbohydrates are used "on-demand" for N_2 fixation to the extent of the nodule mass and the species defined nodule-specific activity. If simulated N-fixation is insufficient because nodule mass is low or temperature is low, then carbohydrates are used for nodule growth, which can result in lags and dynamic pattern of N-fixation and nodule growth. A strong seasonal pattern was observed between the N fixation rate and the cyclic alfalfa regrowth. In fact, the simulated N fixation closely matched the magnitude and life-cycle pattern of the cutting cycle. Alfalfa consistently shows greater amounts of N_2 fixation and percentage N derived from symbiosis than most other legumes species on a seasonal basis. Estimates of N_2 fixation in alfalfa vary from 50 to 463 kg of N_2 fixed ha^{-1} yr^{-1} with about 200 kg of N_2 fixed ha^{-1} yr^{-1} average (Vance, 1978). A dramatic decrease was observed for the simulated nodule weight curve that was related to the N fertilization event during the period May 2016. This behavior is documented by Ghiocel et al. (2013), who studied the impact of N fertilization in alfalfa on nodule formation and N fixation capacity. He reported that the number of nodule sites decreased about 85% and the weight of the nodules decreased significantly from 0.52 g $plant^{-1}$ in the control treatment (no fertilizer) to 0.11 g $plant^{-1}$ and the N_2 fixation rate decreased from 0.78 mg $plant^{-1}d^{-1}$ to 0.02 mg $plant^{-1}d^{-1}$ when fertilized with 100 kg N ha^{-1}. The N_2 fixation rate obtained by Martensson and Ljunggren (1984) ranged between 0.58 and 0.76 kg N ha^{-1} d^{-1}-depending on the method used for the measurement. The average of N_2 fixation rate simulated in the model for the six experiments is 1.5 kg N ha^{-1} d^{-1}. Boote et al. (2008) demonstrated that the nodule growth and N-fixation

subroutines in CROPGRO worked very well for soybean as compared with several data sets.

SUMMARY OF MODEL ADAPTATION AND PERFORMANCE

Adaptation of the CSM-CROPGRO-PFM model for alfalfa was accomplished by changing parameters and relationships describing species tissue compositions, partitioning, and the species' cardinal temperatures for responses of processes to environmental variables. As a first working version, the modified forage version of CROPGRO-PFM for alfalfa marks a significant step in adapting the model to simulate the alfalfa growth and yield. The combination of field experimentation and values reported in the literature has proven to be effective in providing an initially-adapted model but also in identifying future research needs and points of improvement for the model. Parameters may be relatively easily adjusted as new knowledge becomes available. While this adapted model represents progress based on the use of literature information and data from six field experiments in Spain, additional testing and calibration against additional data collected from diverse sites, environments, and treatments are needed to improve the robustness of the model for general use. We conclude that the model gives reasonably realistic responses to seasonal climatic variation and harvest cycles, and can be used as a preliminary tool, awaiting both additional detailed research studies and additional field testing. For example, physiological mechanisms for growth responses in forage plants such as alfalfa would be enhanced by additional specific studies on the dynamics of carbon and N metabolism during regrowth. This CSM-CROPGRO-PFM model version for alfalfa is included in the DSSAT package of crop models and is available as part of the latest version (v. 4.7) (Hoogenboom et al., 2017). Inclusion in the DSSAT V4.7 release will make it available for future testing and improvement. Beyond the goal of model improvement, an important medium-term research challenge in the area of forage crops is to improve the management of systems such that they express their productive potential in a sustainable manner with resilience under a changing climate. A long-term objective of this research is to evaluate best management practices for alfalfa cropping systems under different scenarios of irrigation water availability and climate change.

ACKNOWLEDGMENTS

This work was funded by the Ministry of Economy and Competitiveness of the Spanish Government through the research grants (AGL2013-48728-C2-2-R). We thank this Ministry for awarding Wafa Malik a predoctoral fellowship and financial support for research abroad internship at the University of Florida. Thanks are given to the Almudévar Water User Association and to CSIC/CITA field staff and technicians for their technical support

REFERENCES

Alderman, P.D., K.J. Boote, J.W. Jones, and V.S. Bhatia. 2015. Adapting the CSM-CROPGRO model for pigeonpea using sequential parameter estimation. Field Crops Res. 181:1–15. doi:10.1016/j.fcr.2015.05.024

Antolín, M.C., J. Yoller, and M. Sánchez-Díaz. 1995. Effect of temporary drought on nitrate-fed and nitrogen-fixing alfalfa plants. Plant Sci. 107:159–165. doi:10.1016/0168-9452(95)04108-7

Asseng, S., F. Ewert, C. Rosenzweig, J.W. Jones, J.L. Hatfield, A.C. Ruane, et al. 2013. Uncertainty in simulating wheat yields under climate change. Nat. Clim. Chang. 3:827–832. doi:10.1038/nclimate1916

Avice, J.C., S. Louahlia, A. Kim, A. Morvan-Bertrand, M.P. Prudhomme, A. Ourry, and J.C. Simon. 2001. Influence des réserves azotées et carbonées sur la repousse des espèces prairiales. Fourrages (Versailles) 165:3–22.

Bajaj, S., J. Targolli, L.F. Liu, T.H.D. Ho, and R. Wu. 1999. Transgenic approaches to increase dehydration-stress tolerance in plants. Mol. Breed. 5:493–503. doi:10.1023/A:1009660413133

Barnes, D.K., B.P. Goplen, and J.E. Baylor. 1988. Highlights in the USA and Canada. In: A.A. Hanson, editor, Alfalfa and alfalfa improvement. p. 163–194.

Boller, B.C., and G.H. Heichel. 1984. Canopy structure and photosynthesis of alfalfa genotypes differing in nodule effectiveness. Crop Sci. 24:91–96. doi:10.2135/cropsci1984.0011183X002400010021x

Boote, K.J., G. Hoogenboom, J.W. Jones, and K.T. Ingram. 2008. Modeling N-fixation and its relationship to N uptake in the CROPGRO Model. In: L. Ma, L. Ahuja, and T. Bruulsema, editors, Quantifying and understanding plant nitrogen uptake for systems modeling. Taylor & Francis Group LLC, Boca Raton, FL.

Boote, K.J., M.I. Minguez, and F. Sau. 2002. Adapting the CROPGRO legume model to simulate growth of fababean. Agron. J. 94:743–756. doi:10.2134/agronj2002.7430

Boote, K.J., and N.P. Pickering. 1994. Modeling photosynthesis of row crop canopies. Hortic. Sci. 29:1423–1434.

Boote, K.J., J.W. Jones, G. Hoogenboom, and N.B. Pickering. 1998. The CROPGRO model for grain legumes. In: G.Y. Tsuji, G. Hoogenboom, and P.K. Thornton, editors, Understanding options for agricultural production. Kluwer, Dordrecht, the Netherlands. p. 99–128. doi:10.1007/978-94-017-3624-4_6

Bourgeois, G. 1990. Evaluation of an alfalfa growth simulation model under Quebec conditions. Agric. Syst. 32:1–12. doi:10.1016/0308-521X(90)90026-M

Brisson, N., B. Mary, D. Ripoche, M.H. Jeuffroy, F. Ruget, B. Nicoullaud, et al. 1998. STICS: A generic model for the simulation of crops and their water and nitrogen balances. I. Theory and parameterization applied to wheat and corn. Agronomy 18:311–346. doi:10.1051/agro:19980501

Brown, R.H., and V.E. Gracen. 1972. Distribution of the post-illumination burst among grasses. Crop Sci. 12:30–33. doi:10.2135/cropsci1972.0011183X001200010010x

Bula, R.J. 1972. Morphological characteristics of alfalfa plants grown at several temperatures. Crop Sci. 12:683–686. doi:10.2135/cropsci1972.0011183X001200050039x

Buntin, G.D., and L.P. Pedigo. 1985. Alfalfa development, dry matter accumulation, and partitioning after surrogate insect defoliation of stubble. Crop Sci. 25:1035–1040. doi:10.2135/cropsci1985.0011183X002500060034x

Casella, G., and E.I. George. 1992. Explaining the Gibbs Sampler. Am. Stat. 46:167–174.

Cavero, J., M. Faci, E.T. Medina, and A. Martínez-Cob. 2017. Alfalfa forage production under solid-set sprinkler irrigation in a semi-arid climate. Agric. Water Manage. 191:184–192. doi:10.1016/j.agwat.2017.06.018

Charles-Edwards, D.A., D. Doley, and G.M. Rimmington. 1986. Modelling plant growth and development. Academic Press Inc., Orlando, FL.

Chib, S., and E. Greenberg. 1995. Understanding the Metropolis–Hastings algorithm. Am. Stat. 49:327–335.

Confalonieri, R., and L. Bechini. 2004. A preliminary evaluation of the simulation model CropSyst for alfalfa. Eur. J. Agron. 21:223–237. doi:10.1016/j.eja.2003.08.003

Confalonieri, R., T. Maggiore, and L. Bechini. 2001. Application of the simulation model CropSyst to an intensive forage system in northern Italy, Proceedings of the 2nd International Symposium "Modelling Cropping Systems", Florence, Italy. 16–18 July 2001.

Denison, R.F., and R.S. Loomis. 1989. An integrative physiological model of alfalfa growth and development. Univ. Calif. Div. Agric. Natural Resources. Publ. 1926:73.

Ehleringer, J., and O. Bjorkman. 1977. Quantum yields for CO_2 uptake in C_{-3} and C_{-4} plants dependence on temperature, CO_2, and O_2 concentration. Plant Physiol. 59:86–90. doi:10.1104/pp.59.1.86

FAO. 2003. Food energy – methods of analysis and conversion factors. Technical Workshop on Food Energy – Methods of Analysis and Conversion Factors, Rome, Italy. 3–6 Dec. 2002. FAO, Rome, Italy.

Fick, G.W., D.A. Holt, and D.G. Lugg. 1988. Environmental physiology and crop growth. In: A.A. Hanson, et al., editors, Alfalfa and alfalfa improvement. Agron. Monogr. 29. ASA, CSSA, SSSA, Madison, WI. p. 163–194, doi:10.2134/agronmonogr29.c5.

Fick, G.W. 1981. ALSIM 1 (Level 2) Users manual. Mimeo. 81–35. Cornell University, Dep. Agronomy, Ithaca, NY.

Fox, D., D. Kirby, G.L. Rodney, J. Caton, and K. Krabbenhoft. 1991. Chemical composition of leafy spurge and alfalfa. North Dakota Farm Research Bimonthly Bulletin 48:7–9.

Ghiocel, C., D. Neculai, D. Carmen, S. Rodica, M. Nicoleta, and V. Darius. 2013. Nitrogen fertilisation and nodosity-forming capacity in alfalfa. Scientific Papers: Animal Science & Biotechnologies/Lucrari Stiintifice. Zootehnie si Biotehnologii 46:169–171.

Gijsman, A.J., G. Hoogenboom, W.J. Parton, and C.P. Kerridge. 2002. Modifying DSSAT crop models for low-input agricultural systems using a soil organic matter residue module from CENTURY. Agron. J. 94:462–474. doi:10.2134/agronj2002.4620

Gosse, G., M. Chatier, and G. Lemaire. 1984. Mise au point d'un modèle de prévision de production pour une culture de luzerne. C.R. Acad. Sci. Paris, Ser. III 298:541–544.

Gowgani, G.G. 1977. The effects of termoperiod on growth and development of *Medicago sativa* L. Dissertation Abstracts International B. 37:3235–3236.

Hartkamp, A.D., G. Hoogenboom, R.A. Gilbert, T. Bensond, S.A. Tarawalie, A.J. Gijsman, W. Bowen, and J.W. White. 2002. Adaptation of the CROPGRO growth model to velvet bean (*Mucuna pruriens*): I. Model development. Crops Research 78:9–25. doi:10.1016/S0378-4290(02)00091-6

Hatch, M.D. and C. Slack. 1966. Photosynthesis by sugarcane leaves. A new carboxylation reaction and the pathway of sugar formation. Biochem. J. 101:103–111.

Hatch, M.D., and C. Slack. 1967. Further studies on a new pathway of photosynthetic carbon dioxide fixation in sugar-cane and its occurrence in other plant species. Biochem. J. 102:417–422. doi:10.1042/bj1020417

Hintz, R.W., and K.A. Albrecht. 1991. Prediction of alfalfa chemical composition from maturity and plant morphology. Crop Sci. 31:1561–1565. doi:10.2135/cropsci1991.0011183X003100060036x

Holt, D.A., R.J. Bula, G.E. Miles, M.M. Schreiber, and R.M. Peart. 1975. Environmental physiology, modeling and simulation of alfalfa growth. I. Conceptual development of SIMED. Agric Exp. Sta. Bull. 907. Purdue University, West Lafayette, IN.

Hoogenboom, G., C.H. Porter, V. Shelia, K.J. Boote, U. Singh, J.W. White, et al. 2017. Decision Support System for Agrotechnology Transfer (DSSAT) Version 4.7. https://DSSAT.net. DSSAT Foundation, Gainesville, FL.

Hoogenboom, G., J.W. Jones, P.W. Wilkens, C.H. Porter, K.J. Boote, L.A. Hunt, et al. 2015. Decision Support System for Agrotechnology Transfer (DSSAT) Version 4.6. http://dssat.net. DSSAT Foundation, Prosser, WA. doi.org/10.1080/00288233.2015.1018392

Huffaker, R.C., T. Radin, G.E. Kleinkop, and E.L. Cox. 1970. Effects of mild water stress on enzymes of nitrate assimilation of carboxylative phase of photosynthesis in barley. Crop Sci. 10:471–474. doi:10.2135/cropsci1970.0011183X001000050003x

Huyghe, C. 2003. Les fourrages et la production de protéines. In: Actes des Journées AFPF. Association Française pour la Production Fourragère, Paris, France. p. 3–16.

Jégo, G., C.A. Rotz, G. Belanger, G.F. Tremblay, E. Charbonneau, and D. Pellerin. 2015. Simulating forage crop production in a northern climate with the Integrated Farm System Model. Can. J. Plant Sci. 95:745–757. doi:10.4141/cjps-2014-375

Jeney, C. 1972. The influence of air temperature on the growth and development of lucerne. Takarmany-Bazis 12:19–36.

Jones, J.W., G. Hoogenboom, C.H. Porter, K.J. Boote, W.D. Batchelor, L.A. Hunt, et al. 2003. The DSSAT cropping system model. Eur. J. Agron. 18:235–265. doi:10.1016/S1161-0301(02)00107-7

Jones, J.W., K.J. Boote, G. Hoogenboom, S.S. Jagtap, and G.G. Wilkerson. 1989. SOYGRO V5.42, Soybean crop growth simulation model. User's guide. Florida Agric. Exp. Stn., Univ. of Florida, Gainesville, FL.

Kajala, K., S. Covshoff, S. Karki, H. Woodfield, B.J. Tolley, M.J. Dionora, et al. 2011. Strategies for engineering a two-celled C_4 photosynthetic pathway into rice. J. Exp. Bot. 62:3001–3010. doi:10.1093/jxb/err022

Khaiti, M., and G. Lemaire. 1992. Dynamics of shoot and root growth of lucerne after seeding and after cutting. Eur. J. Agron. 1:241–247. doi:10.1016/S1161-0301(14)80076-2

Lara, M.A.S., C.G.S. Pedreira, K.J. Boote, B.C. Pedreira, L.S.B. Moreno, and P.D. Alderman. 2012. Predicting growth of *Panicum maximum*: An adaptation of the CROPGRO-perennial forage model. Agron. J. 104:600–611. doi:10.2134/agronj2011.0272

Li, R., J.J. Volenec, B.C. Joern, and S.M. Cunningham. 1996. Seasonal changes in nonstructural carbohydrates, protein, and macronutrients in roots of alfalfa, red clover, sweetclover, and birdsfoot trefoil. Crop Sci. 36:617–623. doi:10.2135/cropsci1996.0011183X003600030016x

Liu, Y., L. Wu, J.A. Baddeley, and C.A. Watson. 2011. Models of biological nitrogen fixation of legumes. A review. Agron. Sustain. Dev. 31:155–172. doi:10.1051/agro/2010008

Martensson, A. M. and H. D. Ljunggren. 1984. Nitrogen fixation in an establishing alfalfa (*Medicago sativa* L.) ley in Sweden, estimated by three different methods. Appl. Environ. 48: 702–707.

Maynar, F.H. 1986. La alfalfa Aragón y su mejora de conservación. Pastos. 16:233–257.

Meuriot, F., J.C. Avice, J.C. Simon, P. Laine, M.L. Decau, and A. Ourry. 2004. Influence of initial N reserves and residual leaf area on growth, N uptake, N partitioning and N storage in alfalfa (*Medicago sativa*) during post-cutting regrowth. Ann. Bot. (London) 94:311–321. doi:10.1093/aob/mch144

Milić, D., D. Karagić, S. Vasiljević, A. Mikić, B. Mijić, and S. Katić. 2011. Leaf and stem chemical composition of divergent alfalfa cultivars. Biotechnology in Animal Husbandry 27:1505–1511. doi:10.2298/BAH1104505M

Miller, D. 1994. What's happened to alfalfa winter hardiness. Proceedings of the 18th Forage Production and Use Symposium. Wis. Forage Council, Deforest, WI. p 131–133.

Moot, D.J., J. Hargreaves, H.E. Brown, and E.I. Teixeira. 2015. Calibration of the APSIM-Lucerne model for 'Grasslands Kaituna' lucerne crops grown in New Zealand, New Zealand. J. Agric. Res. 58:190–202. doi:10.1080/00288233.2015.1018392

Murata, Y., J. Iyama, and T. Honma. 1965. Studies on the mechanism on photosynthesis among species. Proc. Crop. Sci. Soc. Japan 34:154–158.

Noquet, C., F. Meuriot, S. Caillot, J.C. Avice, A. Ourry, S.M. Cunningham, and J.J. Volenec. 2003. Short-day photoperiod induces in N uptake, N partitioning and accumulation of vegetative storage proteins in two *Medicago sativa* cultivars. Funct. Plant Biol. 30:853–863. doi:10.1071/FP03099

Onstad, D.W., and G.W. Fick. 1983. Predicting crude protein, in vitro true digestibility, and leaf proportion in alfalfa herbage. Crop Sci. 23:961–964. doi:10.2135/cropsci1983.0011183X002300050035x

Osment, J.V. 1978. Photorespiration, apparent photosynthesis, specific leaf weight, and leaf anatomy of selected alfalfa (*Medicago sativa* L.) clones. Ph.D. diss., University of Arizona, Tucson.

Paquin, R., and P. Lechasseur. 1982. Acclimatation naturelle de la luzerne au froid: II. Variation de la teneur en sucre totaux des feuilles et des collets. Oecol. Plant. 3:27–38.

Pearce, R.B., G.E. Carlson, R.H. Barnes, R.H. Hart, and C.H. Hanson. 1969. Specific leaf weight and photosynthesis in alfalfa. Crop Sci. 9:423–426. doi:10.2135/cropsci1969.0011183X000900040010x

Pearce, R.B., R.H. Brown, and R.E. Blaset. 1968. Photosynthesis of alfalfa leaves as influenced by age and environment. Crop Sci. 8:677–680. doi:10.2135/cropsci1968.0011183X000800060011x

Pedreira, B.C., C.G.S. Pedreira, K.J. Boote, M.A.S. Lara, and P.D. Alderman. 2011. Adapting the CROPGRO perennial forage model to predict growth of *Brachiaria brizantha*. Field Crops Research, Amsterdam 120:370–379. doi:10.1016/j.fcr.2010.11.010

Penning de Vries, F.W.T., A.H.M. Brunsting, and H.H. Van Laar. 1974. Products requirements and efficiency of biosynthesis a quantitative approach. J. Theor. Biol. 45:339–377. doi:10.1016/0022-5193(74)90119-2

Pequeno, D.N.L., C.G.S. Pedreira, and K.J. Boote. 2014. Simulating forage production of Marandu palisade grass (*Brachiaria brizantha*) with the CROPGRO-Perennial Forage Model. Crop Pasture Sci. 65:1335–1348.

Ritchie, J.T., and S. Otter. 1985. Description and performance of CERES-wheat: A user-oriented wheat yield model. ARS Wheat Yield Project, ARS-38. Natural Technology Information Service, Springfield, VA. p. 159–175.

Rotz, C.A., M.S. Corsan, D.S. Chianese, F. Montse, S.D. Hafner, and C.U. Coiner. 2012. The integrated farm system model. References manual, version 3.6. United States Department of Agriculture, University Park, PA.

Rymph, S.J., K.J. Boote, A. Irmak, P. Mislevy, and G.W. Evers. 2004. Adapting the CROPGRO model to predict growth and composition of tropical grasses: Developing physiological parameters. Soil and Crop Science Society of Florida Proceedings, Gainesville 63:37–51.

Sanderson, M.A., J.S. Hornstein, and W.F. Wedin. 1989. Alfalfa morphological stage and its relation to in situ digestibility of detergent fractions of stems. Crop Sci. 29:1315–1319. doi:10.2135/cropsci1989.0011183X002900050045x

Saseendran, S.A., L.R. Ahuja, L. Ma, D. Timlin, C.O. Stockle, K.J. Boote, and G. Hoogenboom. 2008. Current water deficit stress simulations in selected agricultural system models. In: L.R. Ahuja, V.R. Reddy, S.A. Saseendran, and Q. Yu, editors, Response of crops to limited water: Advances in agricultural systems modeling. ASA, CSSA, SSSA, Madison, WI. p. 1–38. doi:10.2134/advagricsystmodel1.c1

Schreiber, M.M., G.E. Miles, D.A. Holt, and R.J. Bula. 1978. Sensitivity analysis of SIMED. Agron. J. 70:105–108. doi:10.2134/agronj1978.00021962007000010024x

Sexton, P.J., W.D. Batchelor, K.J. Boote, and R.M. Shibles. 1998. Evaluation of CROPGRO for prediction of soybean nitrogen balance in a midwestern environment. Trans. ASAE 41:1543–1548. doi:10.13031/2013.17286

Sharratt, B.S., C.C. Sheaffer, and D.G. Baker. 1989. Base temperature for the application of the growing-degree-day model to field grown alfalfa. Field Crops Res. 21:95–102. doi:10.1016/0378-4290(89)90045-2

Sheehy, J.E., and S.C. Popple. 1981. Photosynthesis, water relations, temperature and canopy structure as factors influencing the growth of Sainfoin (*Onobrychis viciifolia* Scop.) and lucerne (*Medicago sativa* L.). Ann. Bot. (London) 48:113–128. doi:10.1093/oxfordjournals.aob.a086105

Simon, J.C., M.L. Decau, J.C. Avice, A. Jacquet, F. Meuriot, and J.M. Allirand. 2004. Effects of initial N reserve status and residual leaf area after cutting on leaf area and organ establishment during regrowth of alfalfa. Can. J. Plant Sci. 84:1059. doi:10.4141/P03-118

Singh, P., and S.M. Virmani. 1996. Modeling growth and yield of chickpea (*Cicerarietinum* L.). Field Crops Res. 46:41–59. doi:10.1016/0378-4290(95)00085-2

Stavarache, M., V. Vîntu, C. Samuil, I. Muntianu, A. Albu, D. Tarcău, C.I. Popovici, and C. Ciobanu. 2012. Quality of alfalfa (*Medicago sativa* L.), in the first year of vegetation. Lucrări Ştiinţifice: Vol. 55/2012, seria Agronomie.

Stavarache, M., C. Samuil, C.I. Popovici, D. Tarcau, and V. Vintu. 2015. The productivity and quality of alfalfa (*Medicago sativa* L.) in Romanian Forest Steppe. Not Bot Horti Agrobo. 43:179–185. doi:10.15835/nbha4319939

Stöckle, C.O., and R.L. Nelson. 1999. CropSyst User's Manual. Biological Systems Engineering Department, Washington State University, Pullman, WA.

Stöckle, C.O., M. Donatelli, and R. Nelson. 2003. CropSyst, a cropping systems simulation model. Eur. J. Agron. 18:289–307.

Teixeira, E.I., J.M. Derrick, and H.E. Brown. 2009. Modelling seasonality of dry matter partitioning and root maintenance respiration in lucerne (*Medicago sativa* L.). Crop Pasture Sci. 60:778–784. doi:10.1071/CP08409

Teixeira, E.I., D.J. Moot, and M.V. Mickelbart. 2007. Seasonal patterns of root C and N reserves of lucerne crops (*Medicago sativa* L.) grown in a temperate climate were affected by defoliation regime. Eur. J. Agron. 26:10–20. doi:10.1016/j.eja.2006.08.010

Thiébeau, P., N. Beaudoin, E. Justes, J.M. Allirand, and G. Lemaire. 2011. Radiation use efficiency and shoot:root dry matter partitioning in seedling growths and regrowth crops of lucerne (*Medicago sativa* L.) after spring and autumn sowings. Eur. J. Agron. 35:255–268. doi:10.1016/j.eja.2011.07.002

Vance, C.P. 1978. Nitrogen fixation in alfalfa: An overview. Proc Eighth Ann Alfalfa Symposium, St. Paul, MN.

Volenec, J.J., S.M. Cunningham, D.M. Haagenson, W.K. Berg, B.C. Joern, and D.W. Wiersm. 2002. Physiological genetics of alfalfa improvement: Past failures, future prospects. Field Crops Res. 75:97–110. doi:10.1016/S0378-4290(02)00020-5

Volenec, J.J., A. Ourry, and B.C. Joern. 1996. A role for nitrogen reserves in forage regrowth and stress tolerance. Physiol. Plant. 97:185–193. doi:10.1111/j.1399-3054.1996.tb00496.x

Wiersma, D.W., and R. Wiederholt. 2007. Alfalfa cutting height to maximize forage yield and quality. University of Wisconsin Extension.

Wilkerson, G.G., J.W. Jones, K.J. Boote, K.T. Ingram, and J.W. Mishoe. 1983. Modeling soybean growth for crop management. Trans. ASAE 26:63–73. doi:10.13031/2013.33877

Willmott, C.J. 1981. On the validation of models. Phys. Geogr. 2:184–194.

Willmott, C.J., S.G. Ackleson, R.E. Davis, J.J. Feddema, K.M. Klink, D.R. Legates, J. Odonnell, and C.M. Rowe. 1985. Statistics for the evaluation and comparison of models. J. Geophys. Res. 90:8995–9005. doi:10.1029/JC090iC05p08995

Wolf, D.D., and R.E. Blaser. 1971. Leaf development of alfalfa at several temperatures. Crop Sci. 11:479–482. doi:10.2135/cropsci1971.0011183X001100040005x

Wolf, D.D., and R.E. Blaser. 1972. Growth rate and physiology of alfalfa as influenced by canopy and light. Crop Sci. 12:23–26. doi:10.2135/cropsci1972.0011183X001200010008x

Zaka, S., E. Frak, B. Julier, F. Gastal, and G. Louarn. 2016. Intraspecific variation in thermal acclimation of photosynthesis across a range of temperatures in a perennial crop. AoB Plants 8:plw035. doi:10.1093/aobpla/plw035